

Experimental analysis of combustion process in SI Engine using ethanol and ethanol-gasoline blend

M. Gailis^{1,2*} and V. Pirs²

¹Riga Technical University, Faculty of Mechanical Engineering, Transport and Aeronautics, Department of Automotive Engineering, Viskalu 36A, LV 1006 Riga, Latvia

²Latvia University of Agriculture, Faculty of Engineering, Motor Vehicle Institute, Liela street 2, LV 3001 Jelgava, Latvia

*Correspondence: maris.gailis@rtu.lv

Abstract. Effect of fuel composition and ignition timing on combustion parameters of spark ignition (SI) port fuel injection (PFI) engine had been studied experimentally. The engine was fuelled with an ethanol and ethanol-gasoline blend E85. The engine was operated at steady speed at 1,500 min⁻¹ and four load points have been used. Minimal ignition timing advance for maximal brake torque (MBT) at stoichiometric air/ fuel ratio for the tested fuels were found. The fuels were tested at their respective MBT timing and gasoline MBT timing. MBT timing was retarded by 8–11% for ethanol and 5–10% for E85 fuel, comparing to gasoline MBT timing. Indicated mean effective pressure (IMEP) was not affected by ignition timing in tested conditions. Maximal cylinder pressure was increased and flame development phase was extended, when gasoline MBT was used with fuels with high ethanol content at tested conditions.

Key words: Spark ignition, MBT, E85, bio fuel, renewable fuel, heat release, burn duration, combustion, IMEP.

INTRODUCTION

Spark ignition (SI) engine can be fuelled with different fuel types. In Baltic States, most common fuels are of fossil origin, such as gasoline and liquefied petrol gas (LPG). There are commercial fuels that are made from or partially contain renewable resources. For SI engine, these so called ‘drop-in fuels’, where bioethanol is blended with gasoline. In Latvia, gasoline with research octane number RON95 contain 5% vol. of anhydrous bioethanol. Gasoline-ethanol blend E85 contain approximately 75...85% vol. of anhydrous bioethanol, depending on season. In contrary to RON95, E85 is suitable as fuel only for specially designed or converted automobiles, commonly known as ‘Flex-fuel vehicles’ (FFV). Primary reason for it is different air-fuel ratio, comparing ethanol and typical gasoline. Fuel supply system material compatibility with ethanol is another issue.

Fuel type conversion of SI engine equipped automobiles is a common practise, particularly in Lithuania and Latvia. For economic reasons, most vehicle fuel type conversions Latvia and Lithuania nowadays are gasoline-LPG conversions. According to report of European Commission (2015), at time of the report there were 1,000 LPG

vehicles in Estonia, 48,368 in Latvia and 210,000 in Lithuania. The conversion to LPG cost up to 600–3,000 EUR for passenger vehicle and is followed by additional regular maintenance costs (European Commission, 2015).

First generation biofuels, such as fatty acid methyl-ester (FAME) and bioethanol, compete with land use for food production. Second generation biofuels are produced from biomass, that cannot be used as food or feed. Production of bioethanol as second generation biofuel, from agricultural waste, has been started at commercial scale in Italy, Spain and other EU countries. Tax incentives for fuel containing high ratio of bioethanol currently are applied several EU countries, including Lithuania and Latvia (European Commission, 2015). Variations in oil price may rise interest for gasoline-E85 conversion of passenger vehicles, equipped with SI engines.

Kotek et al. (2015) investigated injection timing using fuel with high ethanol ratio in SI port injection engine. They found that injection timing adaptation range of original engine control unit (ECU) was limited and additional control unit (ACU) can be successfully used to extend injection pulse and allow operation of the engine, designed for gasoline use, on E85.

Küüt et al. (2011) performed comparative performance tests on test engine, equipped with commercial Flex-fuel adapter. They used regular gasoline, pure ethanol and farmstead bioethanol. Comparing ethanol fuels, higher engine power was observed using ethanol, and higher efficiency was observed in case of farmstead bioethanol.

Čedík et al. (2014) investigated effect of E85 in SI engine on harmful exhaust emissions. Test, using unmodified ECU yielded increased NO_x emissions, comparing to gasoline use, which can be attributed to lean air-fuel mixture. Use of adapter for injection pulse extension resulted in lower NO_x emissions but increase of HC and CO emissions, comparing to use of E85 and gasoline with unmodified ECU. The obtained results can be attributed to poor adaptation of air-fuel mixture in transient conditions and non-optimal ignition advance for E85 fuel.

Costagliola et al. (2013) investigated combustion efficiency and engine-out emissions using instrumented conventional SI engine, using gasoline-ethanol splash blends from E10 up to E85. Air-fuel ratio was kept close to stoichiometric and ignition advance optimized for each type of test fuel. Ignition advance reduced up to 3% with increase in ethanol content in fuel. They reported slightly shorter flame development and main combustion phase for E85 fuel, comparing to other test fuels. Differences in combustion phasing between fuels were reported as insignificant. Thermal load of engine head was not affected by fuel composition. Use of E85 increased global efficiency and significant reduction of regulated exhaust emissions – NO_x, HC and CO. Using E85, aldehyde emissions were increased twice, and benzene emissions reduced by 50%, comparing to gasoline.

Melo et al. (2012) tested combustion and emission characteristics using hydrous ethanol and gasoline blends at different volumetric ratios, up to 100% hydrous ethanol (H100). Ignition advance was knock and exhaust gas temperature limited and increased with increase of ethanol content. Variations in ignition advance between fuels strongly influenced combustion phasing and made difficult to compare and evaluate results. CO and HC emissions were reduced, aldehyde emissions increased with increase of ethanol content. H100 showed highest thermal efficiency among tested blends. Results of NO_x emissions were inconsistent.

Yoon & Lee (2012) studied effects of anhydrous bioethanol on exhaust emissions and engine performance. They performed engine speed sweep at wide open throttle conditions. Ethanol and regular gasoline, both at respective MBT ignition timing was used. Combustion pressure, brake mean effective pressure was increased and brake specific emissions of CO, HC and NO_x were reduced using ethanol, comparing to gasoline. Increased cylinder pressure was explained with increased volumetric efficiency due to high heat of vaporization and heat capacity of ethanol.

Dirrenberger et al. (2014) measured laminar burning velocity of gasoline and gasoline-ethanol blend. They found that ethanol content up to 15% vol. in gasoline blend does not significantly change laminar burning velocity. Ethanol had higher laminar burning velocity, comparing to gasoline. Difference in burning velocity was larger at mixture equivalence ratio from 0.8 to 1.4. Higher laminar burning velocity of ethanol may indicate, that at non-knocking combustion conditions ignition timing should be retarded for ethanol fuel, comparing to regular gasoline.

Literature studies show that use of ethanol or gasoline blends with high ethanol content have potential for rising SI engine thermal efficiency and decreasing of regulated exhaust emissions. Best results were reported, when both air-fuel ratio and ignition timing was controlled and adjusted to match fuel requirements.

It is generally understood, that for normal engine operation air/ fuel ratio (AFR) must be corrected, if gasoline SI engine is being converted to use high ethanol content fuel (Pirs & Gailis, 2013). Various methods for AFR correction are developed and commercialized, employing ethanol concentration sensor (Wang et al., 2008, McKay et al., 2012), exhaust gas oxygen sensor (Ahn et al., 2008) and in-cylinder pressure (Oliverio et al., 2009). Effect of ignition timing less addressed in research, connected with fuel type conversion. Difference between laminar flame speed between ethanol and gasoline diminishes with increase of pressure (Aleiferis et al. 2013), and most the research is performed in wide open throttle (WOT) mode.

The aim of this study is to evaluate effect of non-optimal (gasoline MBT) ignition timing on combustion phasing using ethanol and E85 fuel at stoichiometric AFR and part load steady state conditions. The results provide insight of combustion behaviour of high ethanol content fuels in case when ignition timing is adjusted gasoline use.

MATERIALS AND METHODS

Test Fuels

Two samples of fuel were used in this study – bioethanol-gasoline blend (E85) and neat hydrous bioethanol (E96). E85 was purchased at commercial gasoline station ‘Lukoil’. E96 was obtained from ethanol producer ‘Jaunpagasts Plus’. Properties of test fuels are included in Table 1. Ethanol content was taken from quality certificates. Density was measured using aerometer. Other parameters were found in the literature. Commercial gasoline RON98 in this study was used as reference fuel for finding gasoline MBT timing.

Table 1. Properties of test fuels

Fuel	E85	E96
Ethanol content, % vol.	84.5	96.2
Density at 15 °C, kg m ⁻³	784	792
Research octane number	101.5 ^b	106.0 ^a
Motor octane number	90.1 ^b	87.0 ^a
Lower heating value, MJ kg ⁻¹	29.2 ^b	26.9 ^a
Laminar flame velocity, m s ⁻¹	-	0.39 ^c

^a Heywood (1988); ^b Szybist et al. (2010); ^c Turner et al. (2011).

Research equipment

The experimental setup consisted of spark ignition engine equipped automobile, which was placed on chassis dynamometer, and instrumented for in-cylinder pressure measurement. Fuel consumption was measurement using *AVL KMA Mobile*. Surrounding air temperature during the tests was 20...23 °C and air pressure 101.4...101.6 kPa.

The test automobile was Renault Twingo, model C068 and production year 2003, equipped with manual gearbox. The engine was equipped with port fuel injection and static two coil ignition system. Characteristics the test engine are listed in Table 2. Original engine control unit (ECU) was replaced by user configurable ECU of type VEMS 3.6. Original oxygen sensor was replaced by wideband sensor Bosch LSU 4.2. Oxygen sensor signal was used for closed loop operation at defined air-fuel ratio. Original fuel injectors Siemens DEKA 873774 (fuel flow rate 100 cc min⁻¹ at 3 bar) were replaced by Siemens DEKA 863409 with increased fuel flow rate 182 cc min⁻¹ at 3 bar. Increased fuel supply rate of replaced injectors ensured sufficient fuel amount in case of E85 and E96 fuel. Spray angles for both injector types were similar. The experimental engine setup for cylinder pressure measurement is shown in Fig. 1.

Table 2. Characteristics of test engine (Renault S. A., 1996)

Parameter	Value
Producer and type	Renault D7F 702
Air supply	naturally aspirated
Cylinder setup	4 cylinder, in-line arrangement
Displacement volume, cm ³	1,149
Torque at 2,500 min ⁻¹ , Nm	93
Power at 5,250 min ⁻¹ , kW	43
Piston stroke and bore, mm	76.8 x 69.0
Compression ratio	9.65
Valves per cylinder	2
Opening of inlet valve, CAD ATDC	350
Closing of inlet valve, CAD BTDC	141
Opening of exhaust valve, CAD ATDC	148
Closing of exhaust valve, CAD BTDC	354

To enable fully sequential injection, camshaft position sensor was installed. External fuel tank and pump was used to make fuel change quick and complete. Altered fuel supply and engine control allowed operation and monitoring of the test engine with

any of test fuels at freely selected ignition advance and within necessary fuel–air ratio, which was controlled in closed loop mode.

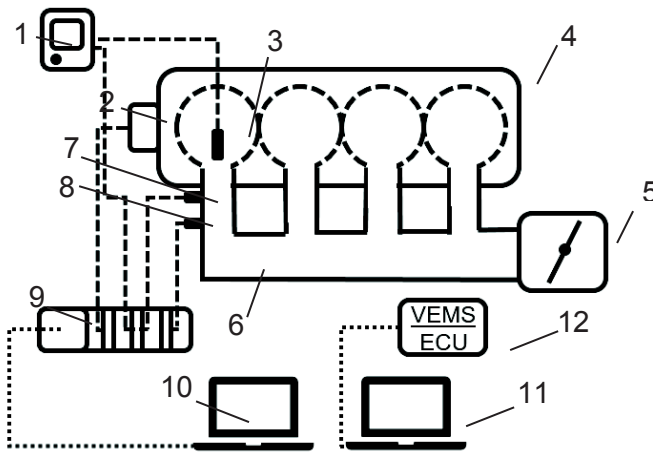


Figure 1. Cylinder pressure measurement setup: 1 – charge amplifier; 2 – crankshaft encoder; 3 – measuring spark plug; 4 – test engine; 5 – adjustable throttle valve; 6 – inlet manifold; 7 – inlet manifold pressure sensor; 8 – temperature sensor; 9 – data acquisition module; 10 – data acquisition control PC; 11 – ECU control PC; 12 – user controllable ECU.

To control inlet manifold pressure and engine load, engine throttle valve was equipped with screw type adjuster.

Engine synchronous measurement of cylinder pressure is taken using modified spark plug with pressure transducer Kistler 6118BD16 and charge amplifier Kistler 5018A. Crankshaft position and speed was detected using optical encoder Kistler 2613B, with resolution 0.1 crank angle degree (CAD). Inlet manifold pressure measurement was taken using GM039 absolute pressure sensor. Inlet air and exhaust gas temperature were measured using K-type thermocouples. Data acquisition was performed using National Instruments equipment, consisting of signal-specific modules and FPGA based controller. Cylinder pressure signal and manifold pressure signal were registered with module NI 9222. Inlet and exhaust temperature was registered using module NI 9214. Crankshaft encoder and camshaft signals were registered using NI 9752 module. Signal-specific modules were installed in NI cRIO 9068 chassis. LabVIEW code was developed, allowing monitoring of cylinder pressure and saving of data. Amplified cylinder pressure signal and manifold pressure sensor signal, synchronized with crankshaft position, and time data were registered in lossless manner with resolution 0.1 CAD.

Chassis dynamometer Mustang MD1750 was used to limit engine speed and absorb power. Dynamometer is equipped with large rollers with diameter 1.27 m and total inertial mass 1148 kg. Power is absorbed using eddy current brake. Combining large inertial mass of the rollers and PID control of the edgy current brake ensured stable rotational speed of the test engine during steady state test conditions.

Test Methodology

Automobile was placed and secured on the chassis dynamometer, engine started and warmed up to nominal coolant temperature at 90 ± 5 °C. Inlet air temperature was held at 42 ± 3 °C and fuel temperature was held at 41 ± 3 °C. Fuel/ air ratio was held close to stoichiometric ratio at all test conditions. Testing was conducted at steady state conditions at selected test points. Selected test points for this report are listed in Table 3. Part load points and engine speed for this report were selected, basing on increased differences in MBT timing for gasoline and ethanol fuels, comparing to conditions of higher engine speed and higher load.

At first stage of the research MBT ignition timing for all three test fuels at all selected test conditions were determined within limits of 0.5 CAD. 50% of cumulative heat release at 10 CAD after piston top dead centre (TDC) was chosen as criteria for MBT timing, according to Heywood (1988). Engine stabilization time at selected conditions before the measurement was 300 s. In case of fuel change engine was run for 1,200 s before measurement was taken. At each test point data of 150 consecutive engine cycles were collected. To statistically evaluate the results, each test was non-consecutively repeated five times.

Table 3. Selected test points

Engine speed, min ⁻¹	Inlet manifold pressure, kPa
1,500	40
	50
	60
	70

Data Processing

MATLAB code for data post processing and report generation was developed. Apparent heat release rate (AHRR) was calculated for each engine cycle using Eq. 1) according to Stone (1999).

$$\frac{dQ_n}{d\varphi} = \frac{\gamma}{\gamma - 1} p \frac{dV}{d\varphi} + \frac{\gamma}{\gamma - 1} V \frac{dp}{d\varphi} \quad (1)$$

where: dQ_n – apparent heat release rate, J deg⁻¹; φ – crank angle degree; γ – ratio of specific heats; V – cylinder volume, m³; p – cylinder pressure, Pa.

To partially compensate heat losses, motoring AHRR was calculated and subtracted from firing AHRR. Mean value of 150 consecutive engine cycles was used as test result.

Ratio of specific heats γ was calculated by finding polynomial fit coefficient for cylinder pressure and volume relation in logarithmic scale. Ratio of specific heats was calculated separately for compression and expansion stroke of each engine cycle and mean value was used for AHRR calculation.

Cumulative heat release (CHR) was calculated using Eq. (2) according to Heywood (1988).

$$Q_n = \int_{\varphi_{start}}^{\varphi_{end}} \frac{dQ_n}{d\varphi} d\varphi \quad (2)$$

where: Q_n – cumulative heat release rate, J.

Relative cumulative heat release (HR) was calculated from CHR and stated in percent. HR was used for combustion phasing analysis. Flame development angle (FDA) was assumed as duration in CAD from spark discharge till 10% of HR. Rapid burning

angle (RBA) was assumed as duration in CAD from 10% till 90% of HR. Overall burning angle was assumed as sum of flame development and rapid burning angle.

Indicated work is calculated using Eq. (3) according to Heywood (1988).

$$W_i = \int_{\varphi_{start}}^{\varphi_{end}} p dV \quad (3)$$

where: W_i – indicated work, J.

Gross indicated work is calculated only in compression and expansion strokes, so gas exchange work is excluded from the result. Indicated mean effective pressure ($IMEP$) is calculated from gross indicated work, using Eq. (4) according to Heywood (1988).

$$IMEP = \frac{W_i}{V_d} \quad (4)$$

where: $IMEP$ – indicated mean effective pressure, bar; V_d – displaced cylinder volume, m³.

RESULTS AND DISCUSSION

The results present burn rate and burn phasing characteristics, using E85 and E96 fuels at MBT timing and for comparison, at gasoline MBT.

Ignition timing

Example of relative cumulative heat release (RCHR) trace is shown in Fig. 2. Lines, labelled ‘MBT’, correspond to fuel’s respective MBT ignition timing. Lines, labelled ‘MBT G’ represent RCHR trace for respective fuel, tested with ignition advance, which matches gasoline MBT. At fuel’s respective MBT, 50% of HR is achieved at 10 CAD after TDC. In case, when E96 and E85 are used with RON98 MBT ignition timing, start of heat release is over advanced for optimal timing. Comparing RCHR trace for all three test fuels at their respective MBT, heat release in case of RON98 appears retarded in late combustion phase, from 40 to 95 CAD.

Table 4. MBT ignition timing at engine speed 1,500 min⁻¹

Inlet manifold pressure, kPa	Test fuel	MBT ignition advance, CAD BTDC
40	E96	27.0
	E85	27.5
	RON98	30.5
50	E96	22.0
	E85	22.0
	RON98	24.0
60	E96	19.5
	E85	19.5
	RON98	21.5
70	E96	18.0
	E85	18.5
	RON98	19.5

Results of experimentally obtained MBT values for test fuels are shown in Table 4. Relatively small difference in MBT timing between E96 and E85 is found at 40 kPa and 70 kPa test conditions. Ignition timing is not limited by detonation, as no detonation was observed.

Results of RCHR trace for other test conditions repeated trend, shown in Fig. 2, and are omitted from this paper for a sake of brevity. The results are discussed in combustion phasing analysis subchapter.

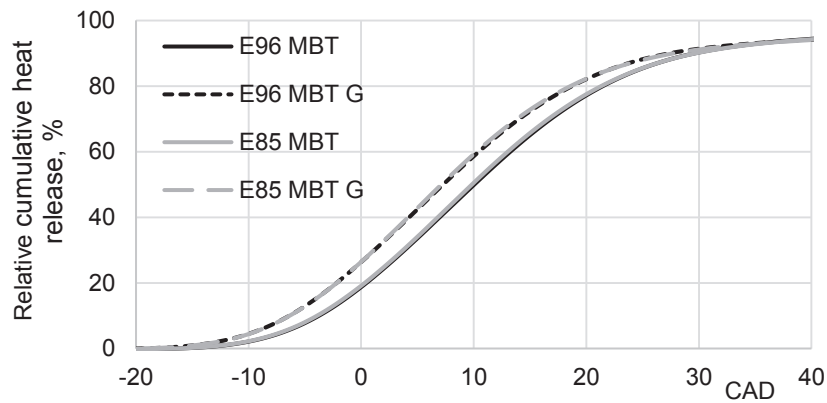


Figure 2. Relative cumulative heat release, engine speed $1,500 \text{ min}^{-1}$, inlet manifold pressure 40 kPa, stoichiometric air/ fuel ratio.

Relative difference of MBT ignition advance for E96 and E85 fuels, comparing to MBT ignition advance for RON98 is shown in Fig. 3.

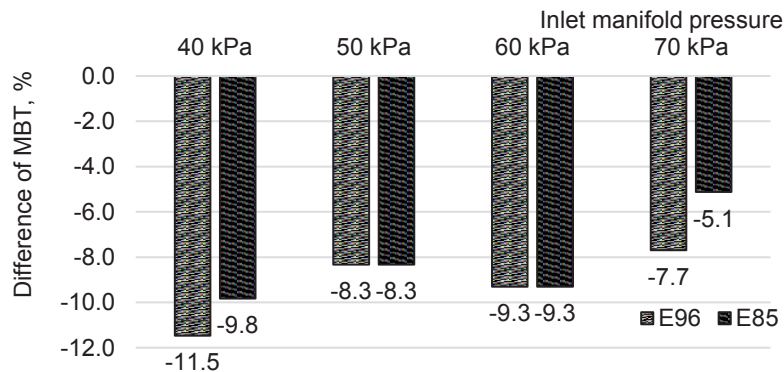


Figure 3. Relative difference of MBT advance, comparing to RON98 MBT, engine speed $1,500 \text{ min}^{-1}$, stoichiometric air/ fuel ratio.

Difference of MBT ignition advance between fuels with high bioethanol content and regular gasoline appears to be decreasing with increase of inlet manifold pressure and thus, increase in charge mass and cylinder pressure. The trend of differences agrees with findings of other researchers (Yücesu et al. 2006; Yoon et al., 2009; Costagliola et al., 2013). The relative difference which is reported in this paper is larger.

Indicated metrics and heat release analysis

Fuel consumption results are shown in Table 5. The data was used for calculation of theoretical energy input for heat release plots.

Fired and motored cylinder pressure trace and AHRR for E96 and E85 in case of inlet manifold pressure 40 kPa are shown in Fig. 4, a and c. MBT spark advance for E96 fuel is 27.0 CAD and 27.5 CAD for E85 fuel. MBT spark advance in case of RON98 is 30.5 CAD. In case where E96 and E85 are fired with ignition timing, which corresponds to gasoline MBT, both fuels show slightly higher AHRR and higher maximal cylinder pressure, comparing to test fuel's MBT timing. At MBT timing maximal cylinder pressure is phased at approximately 16 CAD ATDC. In case of over advanced timing, pressure is rising too early in engine cycle. Greater compression work and unnecessary mechanical stress on the engine parts is expected.

Ratio of specific heats was not significantly affected by ignition advance in tested range. The results are shown in Table 6. Mean value of compression and expansion was used in calculation of heat release.

Cumulative heat release trace and theoretical energy input are shown in Fig. 4, b & d.

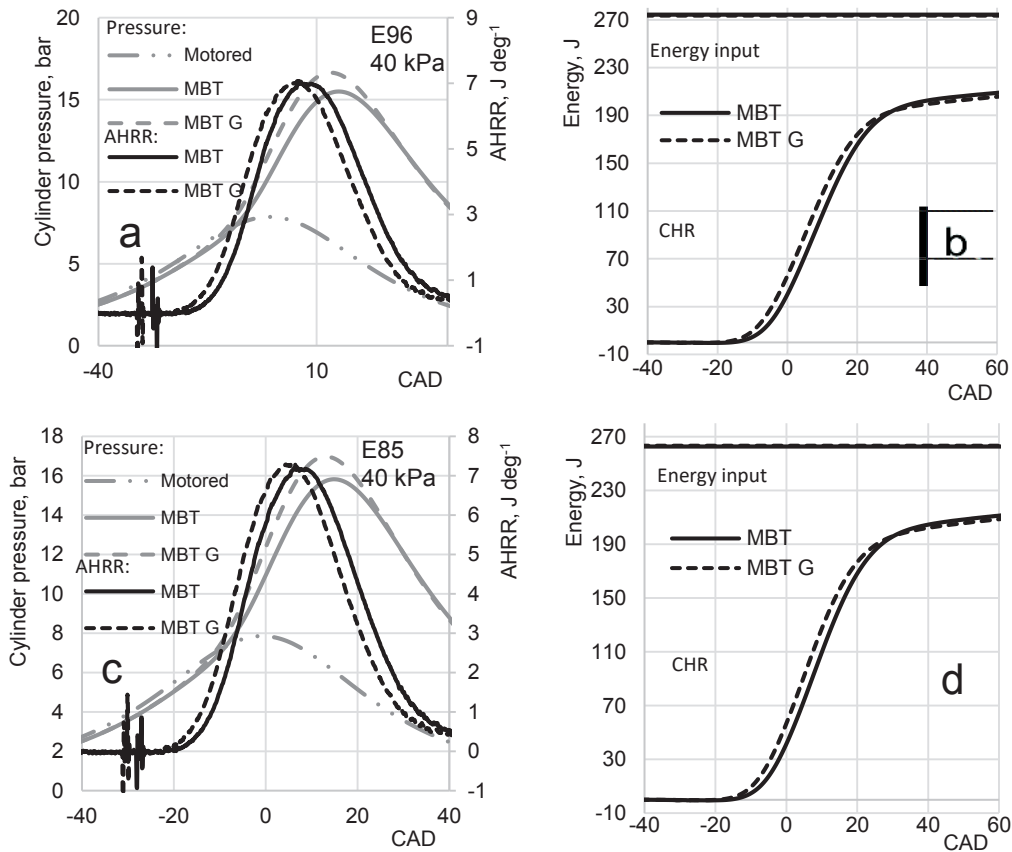


Figure 4. Cylinder pressure, apparent heat release rate and cumulative heat release, inlet manifold pressure 40 kPa. MBT – fuel's MBT timing, MBT G – gasoline MBT timing.

Table 5. Fuel consumption at engine speed 1,500 min⁻¹

Inlet Manifold pressure, kPa	Test fuel	Engine fuel consumption, kg h ⁻¹
40	E96	0.46
	E85	0.41
50	E96	0.61
	E85	0.54
60	E96	0.76
	E85	0.68
70	E96	0.89
	E85	0.79

Table 6. Ratio of specific heats at engine speed 1,500 min⁻¹

Inlet manifold pressure, kPa	Test fuel	Compression	Expansion
40	E96	1.34	1.25
	E85	1.35	1.24
50	E96	1.34	1.25
	E85	1.35	1.24
60	E96	1.34	1.24
	E85	1.35	1.24
70	E96	1.34	1.24
	E85	1.35	1.24

Fired and motored cylinder pressure trace and AHRR for E96 and E85 in case of inlet manifold pressure 50 kPa are shown in Fig. 5, a & c. MBT spark advance for E96 and E85 fuel is 22.0 CAD. MBT spark advance in case of RON98 is 24.0 CAD. Start of heat release and pressure rise is advanced in engine cycle in case of gasoline MBT timing for E96 and E85 fuels, comparing to test fuel's MBT timing.

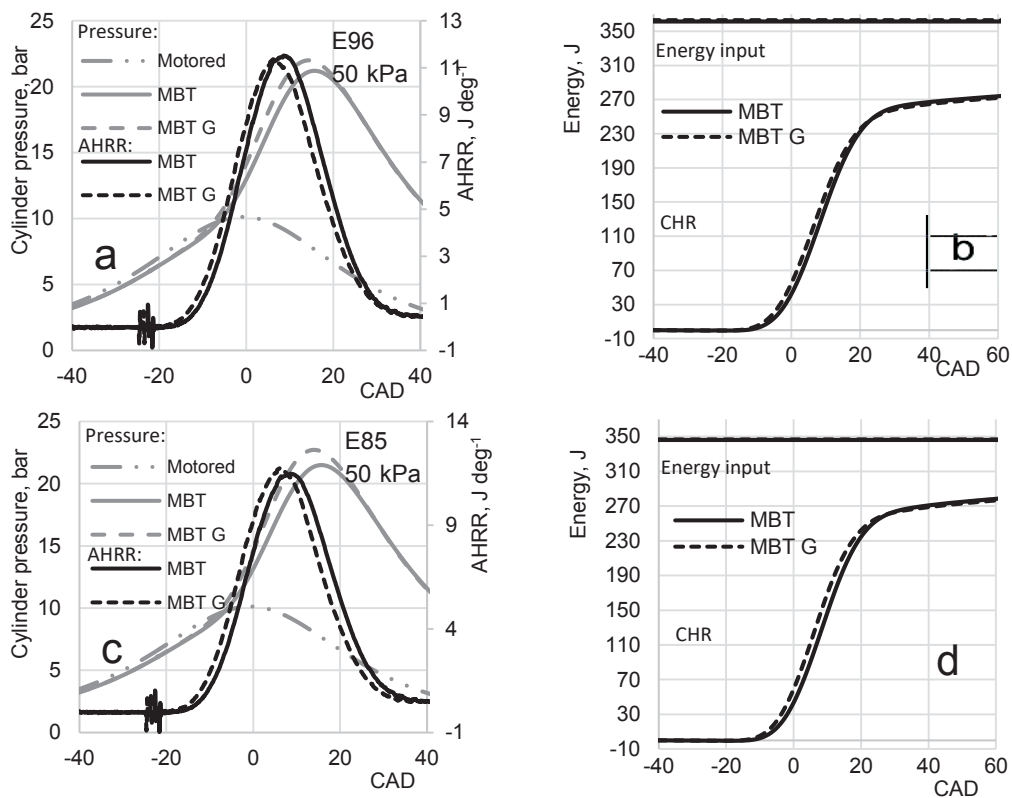


Figure 5. Cylinder pressure, apparent heat release rate and cumulative heat release, inlet manifold pressure 50 kPa. MBT – fuel's MBT timing, MBT G – gasoline MBT timing.

Fired and motored cylinder pressure trace and AHRR for E96 and E85 in case of inlet manifold pressure 60 kPa are shown in Fig. 6, a & c. MBT spark advance for E96 and E85 fuel is 19.5 CAD. MBT spark advance in case of RON98 is 21.5 CAD.

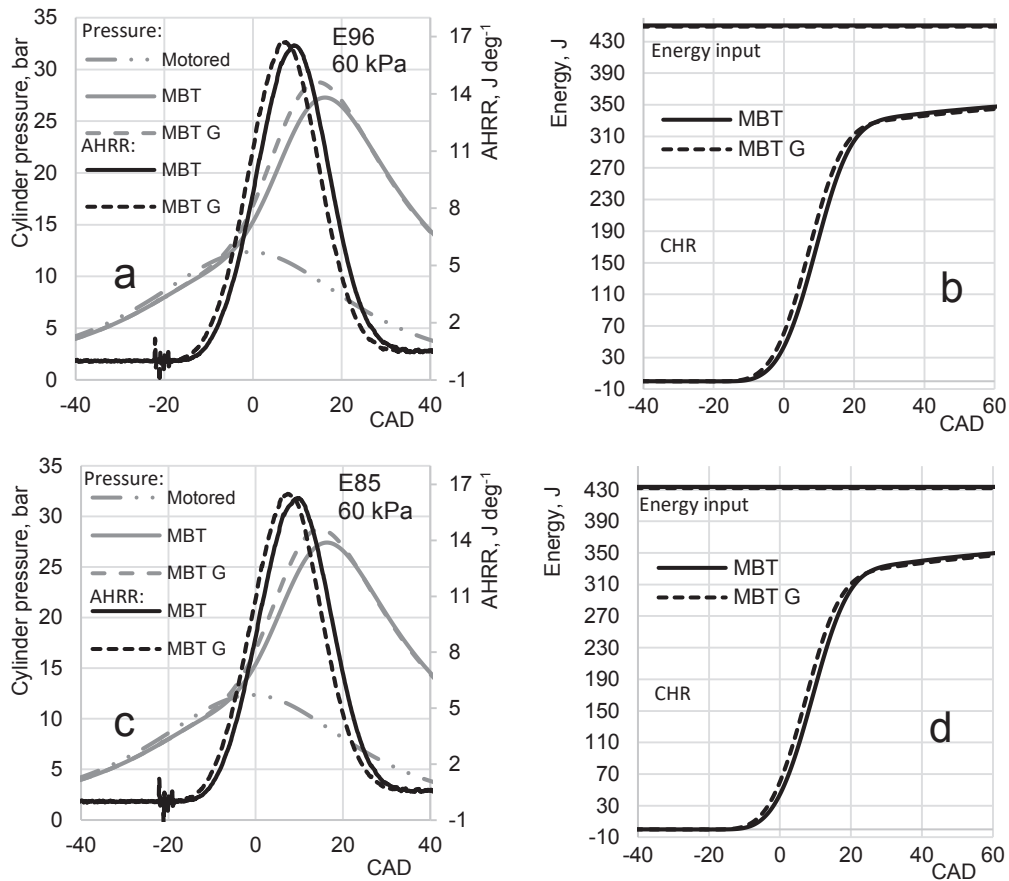


Figure 6. Cylinder pressure, apparent heat release rate and cumulative heat release, inlet manifold pressure 60 kPa. MBT – fuel’s MBT timing, MBT G – gasoline MBT timing.

Fired and motored cylinder pressure trace and AHRR for E96 and E85 in case of inlet manifold pressure 70 kPa are shown in Fig. 7, a & c. MBT spark advance for E96 is 18.0 CAD and for E85 fuel is 18.5 CAD. MBT spark advance in case of RON98 is 19.5 CAD. Difference in MBT timing between fuels with high bioethanol content and pure gasoline is reducing with increase of inlet manifold pressure.

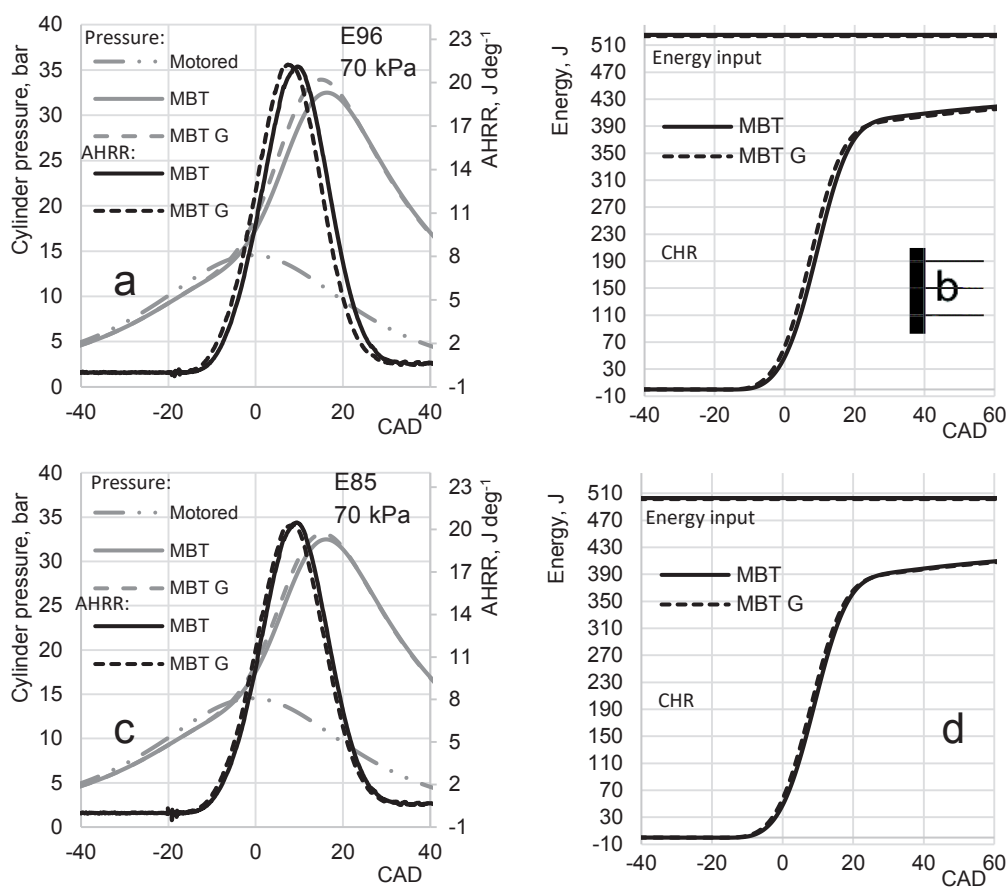


Figure 7. Cylinder pressure, apparent heat release rate and cumulative heat release, inlet manifold pressure 70 kPa. MBT – fuel’s MBT timing, MBT G – gasoline MBT timing.

Maximal cylinder pressure for all test conditions is shown in Fig. 8. Error bars in this and all following diagrams represent confidence interval, calculated with the significance $P = 0.05$. The difference of maximal cylinder pressure is statistically significant, comparing results at fuel’s respective MBT and gasoline MBT. The difference can be attributed to ignition advance but engine temperature and environmental parameters might be influencing factors for maximal cylinder pressure. Increased maximal cylinder pressure may reduce engine life and affect exhaust emissions. Yoon et al. (2009) reported increased maximal cylinder pressure using ethanol, comparing to E85, both set at equal ignition timing. Increase of maximal cylinder pressure was attributed to increased volumetric efficiency caused by charge cooling effect of ethanol. As shown in Fig. 8, no significant differences in maximal cylinder pressure between test fuels were found in this research. Different load control method was used in this research, comparing to Yoon et al. (2009). The authors of this study controlled load by inlet manifold pressure, Yoon et al. (2009) controlled throttle valve position.

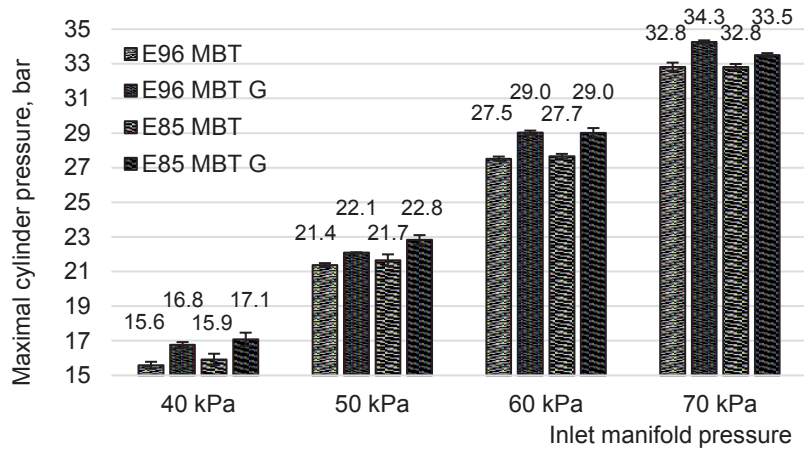


Figure 8. Maximal cylinder pressure at all test conditions.

Effect of variation of ignition advance close to MBT point on engine efficiency is expected to be insignificant. Gross IMEP, calculated for all test conditions, is shown in Fig. 9. Difference of IMEP at fuel's MBT and gasoline MBT is statistically insignificant. IMEP was larger for E85 fuel at test conditions when inlet manifold pressure is from 40 to 60 kPa, comparing to E96 fuel. At test conditions, when inlet manifold pressure is 70 kPa, IMEP is larger for E96 fuel, comparing to E85 fuel.

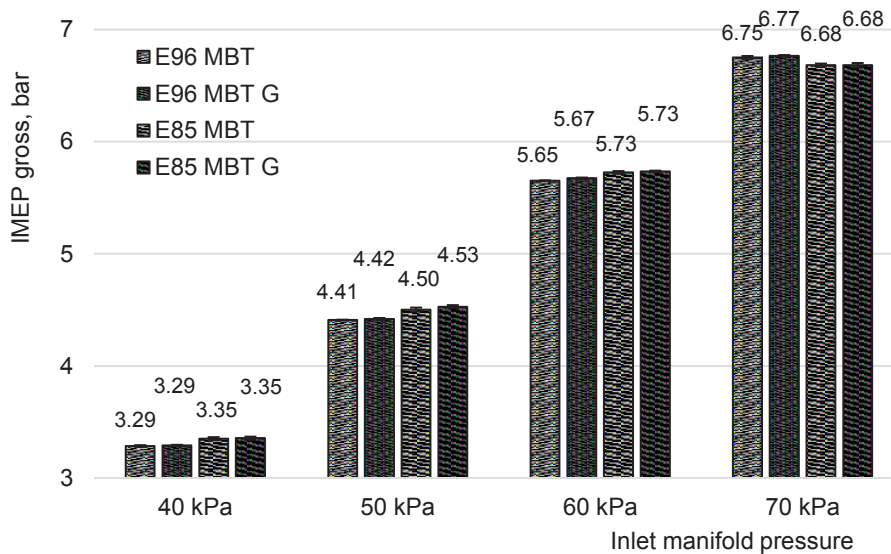


Figure 9. Gross indicated mean effective pressure at all test conditions.

Flame-development angle (FDA) is shown in Fig. 10. It is affected mainly by the mixture composition, pressure, temperature and motion in the close area of the spark plug discharge electrodes. As shown in Fig. 2, during FDA heat is being released at lower rate, comparing to following burning phase. In case of over-advanced ignition

timing (MBT G), flame-development phase is extended in all test conditions for E96 and E85 fuels, comparing to MBT timing. It can be attributed to lower pressure and temperature at the spark discharge in case of MBT G ignition timing. Difference between FDA of specific fuel (E85 or E96) appears to be decreasing with increase of inlet manifold pressure. In case of highest tested load, when inlet manifold pressure is 70 kPa, FDA of E85 appears to be extended, comparing to E96, with both MBT and MBT G ignition timing. The difference is small and statistically insignificant.

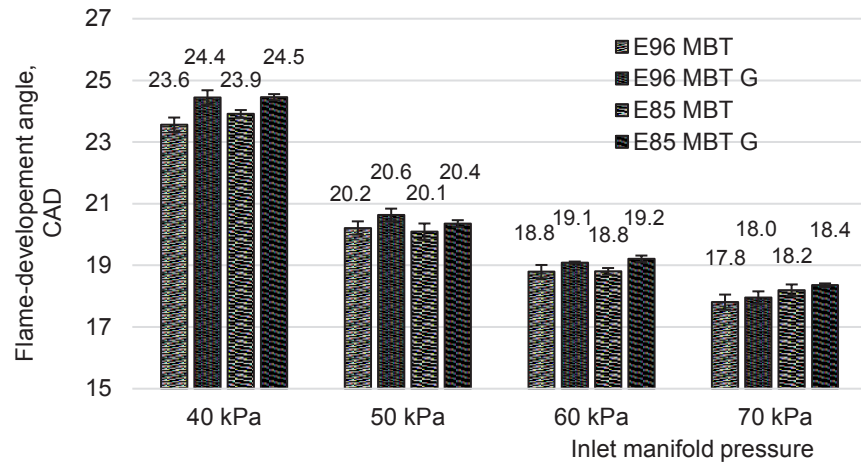


Figure 10. Flame-development angle at all test conditions.

End of flame-development phase is shown in Fig. 11. At MBT timing, flame development end phasing is close for both test fuels. At MBT timing, phasing of 50% of heat release is approximately 16 CAD after TDC. So, duration of heat release between 10% to 50% is approximately the same for both test fuels.

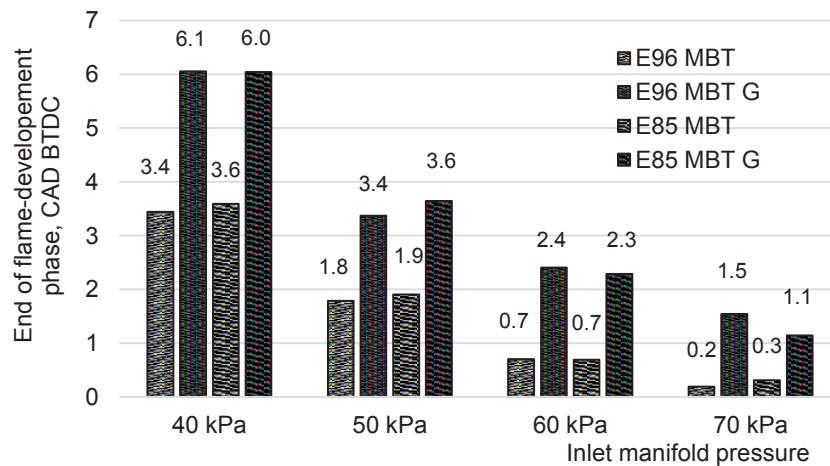


Figure 11. End of flame-development phase at all test conditions.

Combustion analysis, conducted in optically accessible engine using schlieren technique, reveals that at the beginning of combustion flame develops in near spherical form at spark plug electrodes. Surface of flame front is small at the early phase of combustion and it affects energy release rate. As flame front area increases, rate of energy release increases (Heywood, 1988).

In case of MBT G ignition timing, flame-development phase ends early in engine cycle. Comparing to MBT timing, more energy is released before TDC, while cylinder volume is still decreasing. Energy, which is released before TDC, does not contribute to useful work but unnecessary increase in-cylinder pressure. Rapid-burning angle (RBA) is shown in Fig. 12. At low load operating points (40 and 50 kPa), rapid-burning phase (RBP) appears to be extended in case of MBT G spark timing, comparing to MBT timing for both test fuels, but difference is statistically insignificant.

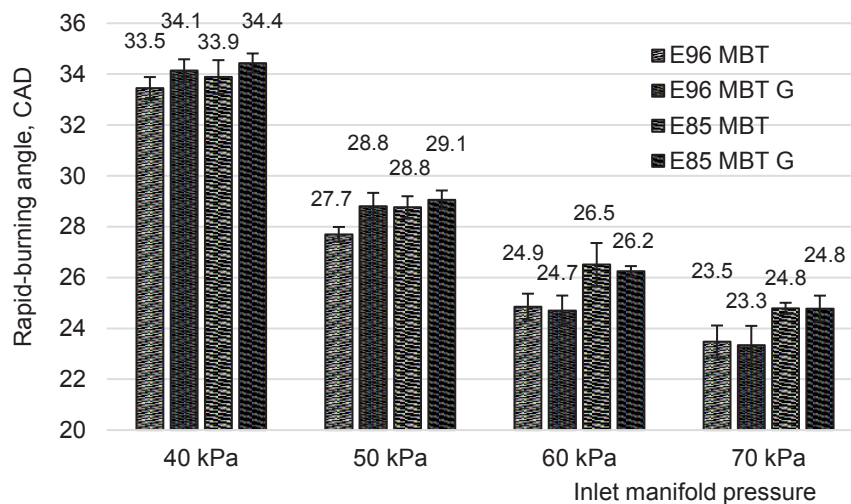


Figure 12. Rapid burn angle at all test conditions.

At higher load (60 and 70 kPa), effect of ignition advance on RBA is small, but difference between test fuels is large and statistically significant, which is in agreement with the findings of Yoon et al. (2009).

As shown in Fig. 11, at higher load (60 and 70 kPa), relatively larger part of RBP is located close to TDC in case of MBT G ignition timing for both test fuels. That may contribute to shorter RBA in those cases, comparing to MBT ignition timing.

Overall burning angle is the sum of FDA and RBA. As major part of combustion occurs during rapid-burning phase, the trend observed in RBA analysis is also present in overall burning angle, which is shown in Fig. 13. As inlet manifold pressure and engine load is increasing, influence of ignition timing is decreasing and influence of fuel chemical and physical properties of fuel is increasing. In case of MBT ignition timing, phasing of 10% and 50% of heat energy release for both test fuels, E96 and E85, are similar. Difference between test fuels increases at late part of combustion, when flame front is reaching combustion chamber wall.

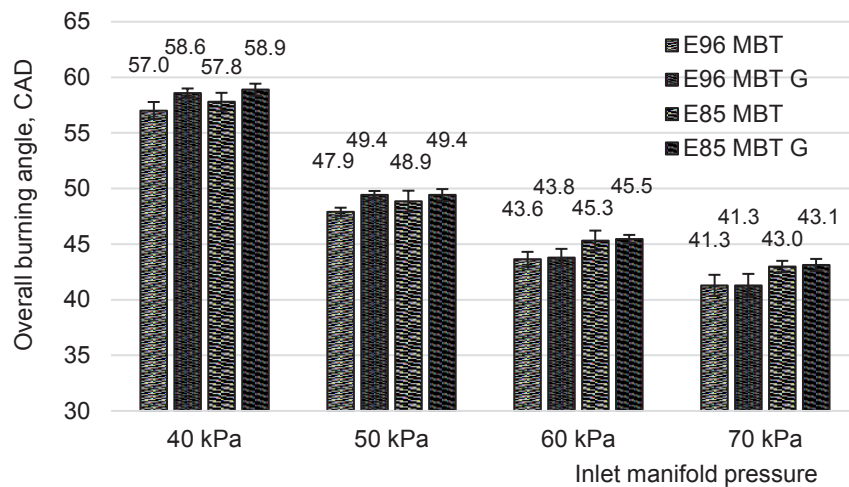


Figure 13. Overall burn angle at all test conditions.

CONCLUSIONS

Hydrous bioethanol and commercial grade ethanol-gasoline blend E85 were tested at steady state operating points using SI PFI engine. Following conclusions from this study can be made:

- MBT timing was retarded for high-ethanol content fuels, comparing to gasoline MBT timing. It can be attributed to faster laminar flame velocity of ethanol and fact, that detonation was not observed at tested conditions.
- Relative difference in MBT timing advance between pure gasoline and high-ethanol content fuels was decreasing with increase in engine load. The effect can be attributed to increasing relative importance of in-cylinder conditions over chemical properties of fuel.
- IMEP was not affected by over-advanced ignition timing in case of gasoline MBT. Increased cylinder pressure did not result in increase of useful engine output work but rather increased mechanical stress on engine parts and changed combustion phasing.
- At low load conditions IMEP was larger for E85 fuel and at highest tested load IMEP was larger for neat hydrous ethanol.
- Flame development angle was increased when gasoline MBT timing was used for high-ethanol content fuels. It can be attributed to lower pressure and temperature at combustion initialization.
- Rapid burning angle was increased at low load conditions when gasoline MBT timing was used for high-ethanol content fuels. Adverse effect was observed at high load conditions. It can be attributed to placement of combustion phases relative to TDC.
- E85 showed extended overall burning angle at high load conditions, comparing to hydrous ethanol. Overall burning angle may affect engine thermal efficiency, engine-out emissions and conditions in exhaust after treatment systems.

The results, presented in this paper are part of larger study on combustion efficiency and exhaust emissions, using and comparing gasoline and high-ethanol content blends. The results provide some insight in effect of fuel composition and ignition timing on combustion phasing in SI PFI engine. The results may be useful in further analysis on requirements and potential benefits of converting gasoline SI engine for high-ethanol content fuel.

REFERENCES

- Ahn, K., Stefanopoulou, A.G. & Jankovic, M. 2008. Estimation of Ethanol Content in Flex-Fuel Vehicles Using an Exhaust Gas Oxygen Sensor: Model, Tuning and Sensitivity. In: *ASME 2008 Dynamic Systems and Control Conference, Parts A and B*. Ann Arbor, p. 8 (In USA)
- Aleiferis, P.G., Serras-Pereira, J. & Richardson, D. 2013. Characterisation of flame development with ethanol, butanol, iso-octane, gasoline and methane in a direct-injection spark-ignition engine. *Fuel* **109**, 256–278.
- Costagliola, A. a., de Simio, L., Iannaccone, S. & Prati, M. V. 2013. Combustion Efficiency and Engine Out Emissions of a S.I. Engine Fueled with Alcohol/Gasoline Blends. *Applied Energy* **111**, 1162–1171.
- Čedík, J., Pexa, M., Kotek, M. & Hromádko, J. 2014. Effect of E85 Fuel on Harmful Emissions – Škoda Fabia 1 . 2 HTP. *Agronomy Research* **12**(2), 315–322.
- Dirrenberger, P., Glaude, P. A., Bounaceur, R., le Gall, H., Pires da Cruz, A., Konnov, A. A. & Battin-Leclerc, F. 2014. Laminar Burning Velocity of Gasolines with Addition of Ethanol. *Fuel* **115**, 162–169.
- Heywood, J.B. 1988. *Internal Combustion Engine Fundamentals*. McGraw-Hill, New York, 930 p.
- Kotek, T., Kotek, M., Jindra, P. & Pexa, M. 2015. Determination of the Optimal Injection Time for Adaptation SI Engine on E85 Fuel Using Self-designed Auxiliary Control Unit. *Agronomy Research* **13**(2), 577–584.
- Küüt, A., Ritslaid, K. & Olt, J. 2011. Study of potential uses for farmstead ethanol as motor fuel. *Agronomy Research Biosystem Engineering Special Issue* **1**, 125–134.
- McKay, B., VanVelzen, I., Guth, C., Achleitner, E. & Biber, P. 2012. An Onboard Ethanol Concentration Sensor for the Brazilian Market. In: *21st SAE Brasil International Congress and Exhibition*. São Paulo, p. 11 (In Brasil)
- Oliverio, N.H., Jiang, L., Yilmaz, H. & Stefanopoulou, A.G. 2009. Modeling the effect of fuel ethanol concentration on cylinder pressure evolution in Direct-Injection Flex-Fuel engines. In: *2009 American Control Conference*. St. Louis, p. 8 (In USA)
- Pirs, V. & Gailis, M. 2013. Research in use of fuel conversion adapters in automobiles running on bioethanol and gasoline mixtures. *Agronomy Research* **11**(1), 205–214.
- Renault S. A., 1996. *Manual de reparation moteur D*. Renault, Bologne-Billancourt, 46 p.
- Melo, T. C., Machado, G. B., Belchior, C. R. P., Colaço, M. J., Barros, J. E. M., de Oliveira, E. J. & de Oliveira, D. G. 2012. Hydrous ethanol–gasoline blends – Combustion and emission investigations on a Flex-Fuel engine. *Fuel* **97**, 796–804.
- State of the Art on Alternative Fuels Transport Systems in the European Union 2015. <http://ec.europa.eu/transport/sites/transport/files/themes/urban/studies/doc/2015-07-alter-fuels-transport-syst-in-eu.pdf>. Accessed 20.1.2017.
- Stone, R. 1999. *Introduction to Internal Combustion Engines*. Third Edition. Palgrave Macmillian, New York . 641 p.
- Szybist, J., Foster, M., Moore, W. R., Confer, K., Youngquist, A. & Wagner, R. 2010, Investigation of Knock Limited Compression Ratio of Ethanol Gasoline Blends. In : *Proceedings of SAE 2010 World Congress & Exhibition*. Detroit, p. 16 (In USA)

- Turner, D., Xu, H., Cracknell, R. F., Natarajan, V. & Chen, X. 2011. Combustion performance of bio-ethanol at various blend ratios in a gasoline direct injection engine. *Fuel* **90**(5), 1999–2006.
- Wang, S.S., Lin, Y., Resendiz, N.H., Granados, Luis E. & Rodriguez, H.H. 2008. Ethanol Concentration Sensor. In: *Proceedings SAE Powertrains, Fuels and Lubricants Meeting 2008*. Detroit, p. 8 (In USA)
- Yoon, S.H., Ha, S.Y., Roh, H.G. & Lee, C.S. 2009. Effect of bioethanol as an alternative fuel on the emissions reduction characteristics and combustion stability in a spark ignition engine. *Proceedings of the Institution of Mechanical Engineers, Part D: Journal of Automobile Engineering* **7**(1), 941–951.
- Yoon, S.H. & Lee, C.S. 2012. Effect of undiluted bioethanol on combustion and emissions reduction in a SI engine at various charge air conditions. *Fuel* **97**(1), 887–890.
- Yücesu, H.S., Topgül, T., Çinar, C. & Okur, M. 2006. Effect of ethanol–gasoline blends on engine performance and exhaust emissions in different compression ratios. *Applied Thermal Engineering* **26**(17–18), 2272–2278.